Insights into structural and dynamical characteristics of III-V boron polytypes

Y. Si Abderrahmane, A. Menad, F. Boutaiba, N. Benyahia, Ali Zaoui, M. Ferhat

Version of Record: https://www.sciencedirect.com/science/article/pii/S1369800121004790
Manuscript_ed9b09331d9628a3b4c255f90b407286

Insights into structural and dynamical characteristics of III-V Boron polytypes

Y. Si Abderrahmane[1], A. Menad[1,2], F. Boutaiba[1], N. Benyahia[1], A. Zaoui[3,*] and M. Ferhat[1]

[1]*Département de Génie Physique, (LPMF). Faculté des Sciences.Université des Sciences et de la Technologie d'Oran, Mohamed Boudiaf. Oran, Algeria*
[2]*Laboratoire de Structure, Elaboration et Application des Matériaux Moléculaires, SEA2M, Université Abdelhamid Ibn Badis, Mostaganem, Algeria.*

[3]*Univ. Lille, Institut Mines-Télécom, Univ. Artois, JUNIA, ULR 4515 – LGCgE, Laboratoire de Génie Civil et géo-Environnement, F-59000 Lille, France*

ABSTRACT

III-V boron materials are a class of semiconductors with a wide range of outstanding properties and applications. In this paper, the density functional theory is used to explore the structural phase stability, atomic structure, electron band structures and dynamics properties of cubic (3C) and hexagonal (2H) polytypes of boron III-V compounds. We show that polytypism has generally a weak impact on electronic and lattice dynamics properties of BP, BAs, BSb, and BBi.

We find small total energy difference between cubic and hexagonal boron-V compounds (~18.7meV/atom, ~15.8meV/atom, ~6.9meV/atom, and ~15.8meV/atom for BP, BAs, BSb and BBi respectively). Accurate quasiparticle (modified Becke-Johnson (mBJ) potential, and local density approximation-1/2) schemes predicted indirect bandgap for 3C and 2H phases of BP, BAs and BSb. Interestingly, BBi evidence narrower direct bandgap for both cubic (~0.38eV) and hexagonal (~0.19eV) crystal polytypes, which makes BBi compound a promising candidate for optoelectronic applications such as infrared sources and detectors. The dynamical stability of 2H boron compounds has also been studied to unravel the possible feasibility of experimental realizations of these compounds. Moreover, we find that the phonon properties of boron III-V compounds contrast considerably with other III-V materials, such the overbending of the transverse optical branches, the bunching of the acoustic branches, the weak LO-TO splitting, and the atypical negative Born effective charges.

Keywords: DFT; III-V Boron semiconductors; crystal polytypes 3C and 2H.

*Email address: azaoui@polytech-lille.fr

I. Introduction

Boron based III-V semiconductors (BP, BAs, BSb, and BBi) and their alloys have recently become highly studied materials in the context of both fundamental investigations and their wide range of possible thermal [1-3], transport [4], and electronic properties [5-29].

BP, BAs, BSb, and BBi usually have the zinc-blende (ZB) crystal structure. Whereas boron nitride (BN), which posses exceptional properties, can stably exists in many polymorphs, such as hexagonal graphite like structure (h-BN), wurtzite-like phase (w-BN), and also cubic diamond-like phase (c-BN). BN share many of its electronic structure properties with group-III nitride compounds (GaN, AlN and InN). For example, BN shows wide gap energies [6, 8, 9, 13, 30, 31], high bulk modulus and elastic constants [9], and a relatively high ionic bonding [32]. In contrast BP, BAs, BSb, and BBi show narrow band gap energies [8, 13, 15, 19], strong covalent bonding [5, 12, 13, 15] and unusual dynamical properties [16] compared to BN.

With the recent progress in nanowires (NWs) growth, a structural novelty was recently demonstrated in semiconductors-NWs based on various cubic-ZB III-V-compounds, which is their unexpected favored crystallization in the hexagonal-wurtzite (WZ) phase. The WZ crystal is not observable at ambient conditions in bulk of any III-V materials except for III-V nitrides.

For instance, a wide number of WZ III-V NWs such as GaAs [33], AlAs [34], GaP[35], InP[36], InAs[37], InSb[38], InGaAs[39], and InAsSb [40] have been grown by modern epitaxial techniques including molecular beam epitaxy (MBE), chemical beam epitaxy, metal organic vapor phase epitaxy (MOVPE), and other techniques. Interestingly, the coexistence of different polytypes (i.e., different crystal phase such as WZ and ZB can coexist in a single NWs) can dramatically modifies the electronic structure properties. For instance indirect ZB semiconductors such as AlAs [34], GaP[35], and GaSbP [41] may evince drastic change of their electronic properties when transformed from the cubic to the wurtzite crystal phase with direct band-gap.

The phenomenon polytypism has been also observed in many II-VI [42-43] and oxide semiconductors such BeO [44] and CaO [45] which crystallizes in the wurtzite structure, unlike the other members of their family (i.e., alkaline-earth oxides: MgO, SrO, and BaO).

In the nanomaterial regime, BN show rich unusual crystalline phases, including, nanotube (1D, BNNTs) [46, 47], hexagonal graphite-like (2D-, h-BN) [48], and 2D nanostructure (including nanosheets [49, 50], nanoribbons [50], and nanomeshes [50]). Moreover, recent DFT calculations addressed the electronic structure properties of two-dimensional hexagonal structure of BN, BP, BAs, and BSb [51], and planar molecules of BN [52-53]. Because of the low dimensionality and the induced confinement effects, 2D B-V materials would offers a plethora of applications. First principles study [51] shows that 2D-h BN, BP, BAs and BSb are mechanically and dynamically stable, and are found semiconductor. Their band-gaps are reduced compared to their 3D-bulk forms, however BN(PB, BAs, BSb) still have wide(narrow) band-gaps. Moreover, 2D-h BN shows strong in-plane stiffness compared to 2D-h BP, BAs, and BSb.

The small ground-state total energy differences (< 25meV) between ZB (3C) and WZ (2H) phase found for III-V phosphides [54], arsenide and antimonide compounds, lead one to ask the question about the stability of boron III-V materials in the WZ phase. Knowledge on the materials properties of the bulk phase of boron compounds is the step towards the optimization of device performances and the design of new Nws-based devices. Moreover, the knowledge regarding WZ electronic structure properties of B-V materials is quite limited in the literature. To address these questions, we present here the detailed calculations of structural, energetic, electronic and dynamical properties of hexagonal WZ-2H polytype phase in comparison to the well-known unstrained ZB-3C structure of III-V boron compounds (BP, BAs, BSb and BBi), using state-of-the-art first-principles pseudopotential calculations.

II. Computational methods

The *ab initio* calculations based on density functional theory (DFT) [55] have been performed using the plane-wave pseudopotential approach as implemented in the Quantum ESPRESSO Package[56]. The exchange-correlation functional of the many-body electron-electron interaction is approximated by its local version, explicitly, the local density approximation (LDA) as parameterized by Perdew and Zunger [57]. Relativistic effects, including spin-orbit coupling (SO) were fully included in the present calculations using the all-electron projector-augmented wave (PAW) scheme [58].

We used a plane-wave cutoff energy of80 Ry, and an energy cut-off of 600 Ry was included for charge density. The Brillouin zone (BZ) was sampled within a 8×8×8 (3C) and 8×8×6 (2H) *k*-points grid according to Monkhorst and Pack [59]. Structural optimizations for cell geometry and atomic positions were performed energy were converged to within 10^{-5} Ry/cell, and the remaining force acting on the atoms are less than 5 10^{-4} RyÅ^{-1}.

The phonon properties are performed using density functional perturbation theory (DFTP)[60]. A 4 × 4 × 4 (3C) and 4 × 4 × 3 (2H) *q*-points MP sampling were employed to perform inverse Fourier transformation.

III. Results and discussions

A. Structural properties

The equilibrium structural parameters of the 3C and 2H polytypes of boron III-V compounds are obtained by minimizing the total-energy with respect to the lattice constant *a* (3C) and the lattice constants *a* and *c* and the internal-cell parameter *u* for the WZ-2H phase. The crystal-polytype types are depicted in Figure 1. The resulting minimum energy surface $E(c, a, u)$ is illustrated in Figure 2.

In Table I, we compare the calculated equilibrium structural parameters of 3C and 2H B-V compounds (V = P, As, Sb, and Bi) with available theoretical and experimental results. The theoretical 3Clattice constants *a* are in excellent agreement with experimental values, being within ~1%, 0.6% and 1.7% of the measured value for BP, BAs and BSb respectively. To the best of our knowledge no experimental data are available for structural parameters of 3C-BBi and 2H boron III-V semiconductors. Nevertheless, the present work is in good agreement with previous calculations [19, 65]. Interestingly, the bulk modulus B_0 is indifferent with crystallographic phase that can adopt boron III-V materials.

The calculated $\frac{c}{a}$ ratio typically deviates from the ideal value of $\sqrt{\frac{8}{3}}\sim1.633$ of III-V metastable WZ semiconductors ($\frac{c}{a}\sim1.645$(GaAs), 1.64(InP), AlP(1.642)) [54]. These findings agree with the empirical rule of Lawartz [66], which states that materials compounds with ZB ground state should have $\frac{c}{a}$ ratios larger than the ideal value of their 'unstable' WZ phase. This rule is also supported by earlier first-principles calculation [42-43, 54] for metastable WZ III-V and II-VI compounds. In addition, the calculated cell-internal parameter *u* for 2H crystal departs from its ideal value $u_0 = \frac{3}{8} = 0.375$. Stable WZ III-V and II-VI compounds show $u>u_0$ [42, 66-67]; while metastable WZ III-V [54] and II-VI [42-43] materials have the opposite trend (i.e., $u<u_0$). We conclude that there is a close correlation between $\frac{c}{a}$ ratio, internal cell parameter *u* and 3C-versus-2H ground-state-stability.

B. Energetic stabilities

The volume dependence of total energy of 3C and 2H polytypes are shown in Figure 3. Clearly the ground state phase of III-V boron compounds is the zinc-blende crystal structure. This means that the cubic (3C) polymorphs are the energetically lowest, agreeing with experimental observations and previous calculations. The stability of the polytype (ZB versus WZ) is described by the total energy difference ΔE between 2H and 3C phases ($\Delta E = E(2H) - E(3C)$). ΔE is ~18.7meV(BP), ~15.8meV(BAs), ~6.9meV(BSb), and ~15.8meV(BBi). From an energetically point of view, the minimum found in ΔE for BSb, compared to BP/BAs/BSb, indicates that WZ BSb crystal can be grown close to equilibrium; whereas that would be relatively more difficult for BP, BAs and BBi. The calculated ΔE agrees well with previous DFT calculations [14] from which 20meV, 15.76meV, 6.74meV, and 15.56meV were derived for BP, BAs, BSb and BBi respectively. The total energy difference ΔE is quite small, thus it costs low energy to change the sequence of the stacking layers 3C→2H, which might be taken as a strong tendency of polytypism in boron III-V compounds. Consequently, under specific temperature and crystal growth conditions, we can expect (or not expect) that BP, BAs, BSb and BBi would have good chance to be synthesized in the wurtzite crystal structure.

C. Electronic structure

It is well known that very often, DFT-LDA fails to predict correctly the energy gaps of semiconductors and insulators, and typically Kohn-Sham gaps underestimates excited states of solids by 50%-100%. The underestimation of the excitation energies is fundamentally attributed to the inherent lack of derivative discontinuity of the exchange-correlation functional. In the last years, an efficient method based on Hedin's GW approximation [68] has been developed [69]. Unfortunately, GW methods are rather computer-time consuming.

The electronic band structure is first performed using the full-potential linearized augmented plane-wave (FP-LAPW) as implemented in the Wien2k code [70] within the recent developed modified Becke-Johnson (mBJ) exchange potential [71] within the LDA. The mBJ exchange potential has been applied to a large variety of solids and was able to deliver accurate excitations energies in close agreement with experiment. In addition, we also apply pseudopotential LDA-1/2 technique [72], which is less computationally expensive, compares well with the popular many-body GW quasiparticle (QP) approach [69] and have shown to work well for a variety of types of semiconductors and insulators [72, 73].

The mBJ band structures, including spin-orbit coupling of B-V compounds in the ZB and WZ crystal structures are displayed respectively in Fig.4 and Fig.5 along the high-symmetry points of the BZ. The various band parameters such as direct and indirect band gaps and spin-orbit coupling are given in Table II (3C) and Table III (2H). All 3C band structures of III-V boron compounds, except BBi, show a minimum of the lowest conduction band near the X point. Earlier QP-GW calculations [8] qualitatively support our findings with minimum indirect(direct) band gaps of 1.90eV (4.4eV) and 1.60eV (4.2eV) for BP and BAs respectively. The calculated fundamental (minimum) band-gaps of ~1.8 eV (BP) and ~1.7 eV (BAs) are in good agreement with the available experimental measurements of ~2 eV for BP [74], and 1.46 ±0.02 eV for BAs [75]. The few existing experimental minimum band gapsfor BSb are probably not reliable, they yield values of 0.46-0.55eV [63] and ~0.51eV [76] close to the earlier underestimated LDA-bandgap calculations of ~0.53eV [11]. The calculated minimum band-gap for BSb is ~0.94eV in good agreement with the recent FP-LAPW calculations [77] in which an indirect-gap of ~1eV was obtained.

The trend concerning the indirect nature of the band-gap of 3C BP, BAs and BSb is violated for BBi. 3C-BBi has a direct band-gap semiconductor at Γ point. Interestingly, the calculated direct narrow energy band gap of 3C-boron bismuth (~0.38eV) corresponds to mid-infrared spectral range of electronic spectrum (λ~3.27μm), which makes BBi a good of choice for many optoelectronic applications such as infrared sources and detectors.

Clearly the band structures of BP, BAs and BSb compounds for 2H and 3C crystals reveal several similarities. All three compounds have indirect band gap. In contrast, all polytypes, the band structure of BBi exhibits a direct band-gap character. 2H-BBi also shows a narrower direct band-gap of ~0.19eV; whereas the indirect gap is ~0.7eV (Γ→M). For 2H polytypes BP, BAs and BSb are also indirect semiconductors, the conduction band minimum is found near the K point for BP and near the M point for BAs ad BSb.

Intriguingly, the indirect band gaps of 3C and 2H polytypes of PB, BAs and BSb are similar. The calculated E_g(ZB)-E_g(WZ) difference is ~0.15eV, ~0.15eV and ~-0.15eV for PB, BAs and BSb respectively. Whereas the direct band gap difference between WZ and ZB crystals highly differs (i.e., E_g(ZB)-E_g(WZ) ~0.7eV(BP), ~0.84eV(BAs) and ~1.14eV(BSb)).

Note that without spin orbit coupling the VB maximum of ZB boron III-V compounds is a threefold degenerate state with Γ_{15v} symmetry. In the presence of the SO coupling, the Γ_{15v} states splits into fourfold-degenerates Γ_{8v} and twofold-degenerate Γ_{7v}. The corresponding $\Delta_{so}(ZB) = \epsilon(\Gamma_{8v}) - \epsilon(\Gamma_{7v})$ is 0.038eV, 0.194eV, 0.324eV and 1.13eV for BP, BAs, BSb

and BBi respectively; whereas $\Delta_{so}(WZ) = \epsilon(\Gamma_{9v}) - \epsilon(\Gamma_{7v})$ is 0.046eV(BP), 0.37eV(BAs), 0.36eV(BSb) and 1.23eV(BBi). The calculated $\Delta_{so}(ZB)$ are close to FLAPW-calculations [78] of 0.041eV, 0.216 eV and 0.366 eV for BP, BAs and BSb respectively. Clearly the strength of Δ_{so} is rather insensitive with respect to polytype structure.

For all polytypes, the SO splitting increase monotonically when anion atomic number increases, i.e., along the anion row P→As→Sb→Bi. However, the SO coupling for B-V materials is significantly smaller than that for their corresponding common-anion compounds ($\Delta_{so}(ZB) = 0.086$ eV(GaP), 0.34 eV(GaAs), 0.73eV(GaSb), 2.15eV(GaBi))[78], because boron III-V semiconductors show stronger covalent bonds compared to other III-V materials[5-6, 10-13, 15].

D. Dynamical properties

The phonon dispersion curves and phonon density of states (PhDoS) for boron compounds in the 3C and 2H crystal phases are illustrated respectively in Fig.6 and Fig.7. The phonon frequencies at high-symmetry points are displayed in Table IV (3C) and TableV (2H). The phonon spectra of boron-V compounds have atypical characteristics when compared to other III-V materials. This can be outlined as follows: (i) Longitudinal (LO) and transverse (LO) optical branches are not clearly separated, in particular for BP and BAs, which is typical for IV-IV semiconductors but not for III-V compounds. (ii) The TO-phonon branches overbend at the X (3C) and M(2H) points for BAs, BSb and BBi, i.e., region in the BZ where the LO mode has higher frequency than at zone-center Γ point. (iii) Bunching of the acoustic branches around K point, contrasting from what occurs for III-V group semiconductors, i.e., the acoustic branches are closer to each other. (4i) Unusual weak LO-TO (3C) splitting at Γ point, with gap-frequencies of ~7cm^{-1}, 3.7cm^{-1}, ~17cm^{-1} and ~8cm^{-1} for BP, BAs, BSb and BBi respectively. These unusual features are related to the strong covalent bonding of boron-V family.

The phonon spectrum of c-BN [32] is very different from those of BP, BAs, BSb, and BBi due to nearly equal mass of B and N atoms. For c-BN, there is no clear gap between acoustic and optical phonon modes, moreover, there is no sharp peak in the PhDoS due to the LO phonon modes, and the transverse acoustic (TA) branches are not flat. For cubic BP, BAs, BSb, and BBi, the reverse is true.

The calculated (3C) TO (~821cm^{-1}) and LO (~828cm^{-1}) values for BP agree well with experimental values of ~820cm^{-1}(TO) [79], ~834cm^{-1} (LO) [79], and~829cm^{-1} (LO) [80].

Moreover, Raman peaks located at ~595 cm^{-1}[63] could be associated to LO phonon mode for 3C-BSb.

The calculated 2H phonon band structure of boron III-V semiconductors (Figure 7) have no soft imaginary phonon frequencies in the whole BZ, suggesting the dynamical stability of wurtzite crystal phase of B-V compounds. The Raman active E_2(high), which can be used for distinguishing the two polytypes 3C and 2H, is about ~777cm^{-1}, ~673cm^{-1}, ~595cm^{-1} and ~517cm^{-1} for BP, BAs, BSb and BBi respectively. The L point in the BZ is folded onto the Γ point in the 3C BZ of the 2H, thus reducing the LO, TO, LA and TA phonon modes at L point of the BZ (3C) to respectively B_1^H, E_2^H, B_1^L and E_2^L at Γ point of the BZ in 2H phase.

According to the above, the estimated value of B_1^H, E_2^H, B_1^L and $E_2^L$are in close agreement with calculated modes of Table V, i.e., the deviation does not exceed ~0.6% for B_1^H,~1% for E_2^H, ~0.4% for B_1^L, and ~4% for E_2^L. By considering the splitting at Γ point, $\Delta w(E_1, A_1) = w(\text{LO})\text{-}w(\text{TO})$, we found for $\Delta w(E_1(A_1))$ mode : ~7cm^{-1} (~8cm^{-1}) for BP, ~5cm^{-1} (~4cm^{-1}) for BAs, ~17cm^{-1} (~18cm^{-1}) for BSb, and ~9cm^{-1} (~10cm^{-1}) for BBi. 2H boron III-V compounds show rather weak LO-TO splitting compared to high ionic 2H III-V nitrides ($\Delta w(E_1)$=~232 cm^{-1} for AlN[81], $\Delta w(E_1)$=~228 cm^{-1} for BN[32]) and metastable 2H III-V materials ($\Delta w(E_1)$ =51cm^{-1} (AlP)[82]). Once again the calculated weak $\Delta w(E_1, A_1)$ for 2H-borides may be related to the strong bonding behavior of these compounds.

As found for the cubic B-V compounds, lattice dynamics of h-BN and boron family differs considerably, in particular h-BN[32], and shows a considerable overlap between the acoustic and optical phonon branches, and flatness of the optical modes (i.e., there is only one clear peak in the PhDoS).

The ratio $\frac{w_{TO}(E_1)-w_{TO}(A_1)}{w_{TO}(E_1)}$ can be used as a measure of the strength of crystal anisotropy of WZ crystal, for which the obtained values are 0.012(BP), 0.008(BAs), 0.009(BSb) and 0.01(BBi). Therefore 2H boron III-V materials evidence weak crystal anisotropy.

To deal with the macroscopic electric field associated with atomic displacements in polar semiconductors, we report in Table VI, the Born effective charge (BEC) $Z^*$and high-frequency dielectric $\varepsilon(\infty)$ tensors for B-V compounds. In the case of 3C polytype, $\varepsilon(\infty)$ (Z^*) has a diagonal form and possesses only one independent component. For the 2H crystal phase, $\varepsilon(\infty)$ (Z^*) is composed of two independent components: one corresponding to the direction parallel to the c axis (||), and the other being characteristic for the hexagonal plane perpendicular to the c axis (⊥). The average $\varepsilon(\infty) = \frac{1}{3}Tr\varepsilon(\infty)\left[Z^* = \frac{1}{3}TrZ^*\right]$ is also reported.

The III-V boron exhibit rather striking and unusual properties, and appear to be very different from conventional III-V semiconductors. Several features of the data in Table VI confirm this statement. (i) B-V compounds display negative BEC value, unlike trends observed in III-V compounds (i.e., Z^*(GaAs) =2)[82]. (ii) Although Z^* have no rigorous relation to nominal ionicity, the ratio $\frac{|Z^*|}{Z_{ion}}$ (where $Z_{ion} = 3$ is the nominal ionic charge) is weak (0.2(BP), 0.17(BAs), 0.43(BSb), and 0.37 for BBi) compared to III-V compounds (~0.66 (GaAs)) [82] and strong (~0.94 (InN) [81], ~0.64 (BN) [32]) ionic III-nitrides compounds. Note that these compounds 'violated' chemical intuition, instead to be the 'cation', boron atom plays the role of 'anion' with respect to the calculated effective charge in BP, BAs, BSb and BBi.

Moreover, 2H B-V compounds show weak anisotropy in their Z^* ($\Delta Z^* = \frac{\left[Z_{\parallel}^* - Z_{\perp}^*\right]}{Z^*}$) and $\varepsilon(\infty)$($\Delta\varepsilon(\infty) = \frac{\left[\varepsilon_{\parallel}(\infty) - \varepsilon_{\perp(\infty)}\right]}{\varepsilon(\infty)}$). Z^* is weakly sensitive to polytypism, since the Z^* value of B-V compounds for both WZ and ZB structures are rather similar, and they differ by less than ~0.1% for BP and BAs, and ~6% for BSb, and BBi.

Finally, we calculate the spontaneous polarization P_s of 2H-crystal structures of B-V compounds within the modern Berry-phase approach [83]. Our calculations give P_s (10^{-3}C/m^2) = 14.84, 8.75, 12.0, 9.76 for BP, BAs, BSb and BBi respectively. Apart BP, 2H boron compounds show modest P_s compared to 2H III-V nitrides compounds such as AlN (-40 10^{-3} C/m^2))[84], and BN (-32 10^{-3} C/m^2))[85], but reveal comparable spontaneous polarization with 'unstable' 2H III-V compounds (P_s = 7 10^{-3}C/m^2 for AlP) [84]. The relatively large value of P_s found for BP can be related to volume effect [67], accounted by $1/a^2$. In particular, the lattice constant of BP is weaker than those of typical III-V compounds.

IV. Conclusion

To summarize, we have presented a first-principles study regarding structural phase stability, electronic, and lattice dynamics properties of boron III-V compounds in the cubic zinc-blende (3C) and hexagonal wurtzite (2H) crystal phases. There is a small total energy difference between 3C and 2H polytypes, suggestinga tendency of polytypism in boron III-V materials. Accurate electronic band structures including spin-orbit coupling has been calculated using the modified Becke-Johnson exchange potential. The excited states are in close agreement with available experimental measurements. BP, BAs, and BSb polytypes have indirect band gap. However, heavier BBi compound evidences direct nature of the band gap in both 3C and 2H crystal polytypes, with a narrower gap-energies of (~0.38eV) (3C) and (~0.19eV) (2H), which makes BBi compounds promising candidates for optoelectronic applications such as infrared sources and detectors.

The lattice dynamics of boron III-V contrast noticeably that of other III-V compounds such as the overbending of transverse optical branches and bunching of acoustic branches. Moreover, contrary to most III-V semiconductors, 3C and 2H boron III-V materials manifest weak LO-TO splitting. Finally, the marked covalent bonding of these compounds yields atypical negative Born effective charge as well as dielectric isotropy of the 2H crystal.

References

[1] L. Lindsay, D. A Broido, and T. L. Reinecke, Phys. Rev. Lett. **111**, 025901 (2013).

[2] L. Lindsay, D. A. Broido, J. Carrete, N. Mingo and T. L. Reinecke, Phys. Rev. B **91**, 121202 (R) (2015).

[3] S. Li, K. M. Taddei, X. Wang, H. Wu, J. Neuefeind, D. Zackaria, X. Liu, C. D. Cruz, and B. Lv, Appl. Phys. Lett. **115**, 011901 (2019).

[4] T.-H. Liu, B. Song, L. Meroueh, Z. Ding, Q. Song, J. Zhou, M. Li, and G. Chen, Phys. Rev. B **98**, 081203 (R) (2018).

[5] R. M. Wentzcovitch, and M. L. Cohen, J.Phys. C: Solid State Phys. **19**, 6791 (1986).

[6] R. M. Wentzcovitch, K. J. Chang and M. L. Cohen, Phys. Rev. B **34**, 1071 (1986).

[7] C. Prasad, and M. Sahay, phys. stat. sol. (b) **154**, 201 (1989).

[8] M. P. Surh, S. G. Louie, and M. L. Cohen, Phys. Rev. B **43**, 9126 (1991).

[9] P. Rodríguez-Hernández, M. Gongález-Diaz and A. Muñoz, Phys. Rev. B **51**, 14705 (1995).

[10] M. Ferhat, A. Zaoui, M. Certier, and B. Khelifa, Phys. Status Solidi b **195**, 415 (1996).

[11] M. Ferhat, B. Bouhafs, A. Zaoui, and H. Aourag, J. Phys.: Condens. Matter **10**, 7995 (1998).

[12] A. Belabbes, A. Zaoui, M. Ferhat, Journal of Physics: Condensed Matter 20, 415221-415224 (2008).

[13] A. Zaoui, and F. El Haj Hassan, J. Phys.: Condens. Matter **13**, 253 (2001).

[14] S. Q. Wang, and H. Q. Ye, phys. stat. sol. (b) **240**, 45 (2003).

[15] A. Zaoui and M. Ferhat, Physica Stat. Sol. (b) 225, 15 (2001).

[16] D. Touat, M. Ferhat, and A. Zaoui, J. Phys.: Condens. Matter **18**, 3647 (2006).

[17] K. Bouamama, P. Djemia, N. Lebga, and K. Kassali, High Pressure Research **27**, 269 (2007).

[18] M. Briki, M. Abdelouhab, A. Zaoui and M. Ferhat, Sup. and Micro. **45**, 80 (2009).

[19] M. Ustundag, M. Aslan, and B. G. Yalcin, Comp. Mat. Sci. **81**, 471 (2014).

[20] W. Shan, W. Walukiewicz, J. Wu, K. M. Yu, J. W. Ager III, S. X. Li, E. E. Haller, J. F. Geisz, D. J. Friedman, and S. R. Kurtz, J. Appl. Phys. **93**, 2696 (2003).

[21] S. Azzi, A. Zaoui, and M. Ferhat, SolidState Commun. **144**, 245 (2007).

[22] N. Hossain, T. J. C. Hosea, S. J. Sweeney, S. Liebich, M. Zimprich, K. Volz, B. Kunert, and W. Stolz, J. Appl. Phys. **110**, 063101 (2011).

[23] A. Ektarawong, S. I. Simak and B. Alling, Phys. Rev. B **96**, 024202 (2017).

[24] H. Ma, J. Zhang, B. Zhao, Q. Wei, and Y. Yang, AIP ADVANCES**7**, 065007 (2017).

[25] J. –X. Shen, D. Wickramaratne, and C. G. Van de Walle, Phys. Rev. Mat. **1**, 065001 (2017).

[26] C. M. Krammel, L. Nattemrann, E. Sterzer, K. Volz, and P. M. Koenraad, J. Appl. Phys. **123**, 161589 (2018).

[27] L. Williams and E. Kioupakis, Appl. Phys. Lett. **111**, 211107 (2017).

[28] H. Maiz Hadj Ahmed, H. Benaissa, A. Zaoui, and M. Ferhat, Phys. Lett. A, **383**, 1385 (2019).

[29] E. Zdanowicz, D. Lida, L. Pawlaczyk, J. Serafinczuk, R. Szukiewicz, R. Kudrawiec, D. Hommel, and K. Ohkawa, J. Appl. Phys.**127**, 165703 (2020).

[30] D. M. Hoffman, G. L. Doll and P. C. Eklund, Phys. Rev. B **30**, 6051 (1984).

[31] G. Satta, G. Cappellini, V. Olveano, and L. Reining, Phys. Rev. B **70**, 195212 (2004).

[32] K. Karch and F. Bechstedt, Phys. Rev. B **56**, 7404 (1997).

[33] I. Zardo, S. Conesa-Boj, F. Peiro, J. R. Morante, J. Arbiol, E. Uccelil, G. Abstreiter, and A. F. i Morral, Phys. Rev. B **80**, 245324 (2009).

[34] S. Funk, A. Li, D. Ercolani, M. Gemmi, L. Sorba, and I. Zardo, ACS Nano **7**, 1400 (2013).

[35] S. Assali, I. Zardo, S. Plissard, D. Kriegner, M. A. Verheijen, G. Bauer, A. Meijerink, A.Belabbes, F. Bechstedt, J. E. M. Haverkort, E. P. A. M. Bakkers, Nano Lett.**13**, 1559 (2013).

[36]N. Vainorius, S. Lehmann, K. A. Dick, and M. –E. Pistol, Optics EXPRESS**28**, 11016 (2020).

[37] I. Zardo, S. Yazji, N. Hörmann, S. Hertenberger, S. Funk, S. Mangialardo, S. Morkötter, G. Koblmüller, P. Postorino, and G. Abstreiter, Nano Lett.**13**, 3011 (2013).

[38] D. Kriegner, C. Panse, B. Mandl, K. A. Dick, M. Keplinger, J. M. Persson, P. Caroff, D. Ercolani, L. Sorba, F. Bechstedt, J. Stangl, and G. Bauer, Nano Lett.**11**, 1483 (2011).

[39]K. W. Ng, W. S. Ko, F. Lu, and C. J. C.-Hasnain, Nano Lett.**14**, 4757 (2014).

[40] H. Potts, M. Friedl, F. Amaduzzi, K. Tang, G. Tütüncüoglu, F. Matteini, E. A. Lladó, P. C. McIntyre and A. F.i Morral, Nano Lett.**16**, 637 (2016).

[41] H. B. Russell, A. N. Andriotis, M. Menon, J. B. Jasinski, A. M.–Garcia, and M. K. Sunkara, Sci.Rep.**6**, 20822; doi:10.1038/srep20822 (2016).

[42] C. –Y. Yeh, Z. W. Lu, S. Froyen, and A. Zunger, Phys.Rev. B 46, 10086 (1992).

[43] F. Boutaiba, A. Belabbes, M. Ferhat, and F. Bechstedt, Phys. Rev. B**89**, 245308 (2014).

[44] D. Li, P. Zhang, and J. Yan, Sci. Rep. **4**, 4707 (2014).

[45] N. Hammou, A. Zaoui and M. Ferhat, J. Alloys and Compounds**815**, 152424 (2020).

[46] N. G. Chorpa, R. J. Luyken, K. Cherrey, V. H. Crespi, M. L. Cohen, S. G. Louie, and A. Zettl, Science **269**, 966 (1995).

[47] T. H. Ferreira, M. C. Miranda, Z. Rocha, A. S. Leal, D. A. Gomes, and E. M. B. Sousa, nanomaterials, **7**, 82 (2017).

[48] L. Song, L. Ci , H. Lu, P. B. Sorokin, C. Jin, J. Nie, A. G. Kvsahnin, D. G. Kvsahnin, J. Lou, B. I. Yakobson, and P. M. Ajayan, Nano Lett.**10**, 3209 (2010).

[49] J. N. Coleman, et al.Science **331**, 568 (2011).

[50] Y. Lin and J. W. Connell, Nanoscale**4**, 6908 (2012).

[51] H. Şahin, S. Cahangirov, M. Topsakal, E. Bekaroglu, E. Akturk, R. T. Senger, and S. Ciraci, Phys. Rev. B**80**, 155453 (2009).

[52] P. Mocci, R. Cardia, and G. Cappellini, Phys. Chem. Chem. Phys.**21**, 16302 (2019).

[53] P. Mocci, R. Cardia, A. Bosin, and G. Cappellini,J. of Phys: Conference Series, **1548**, 012028 (2020).

[54] F. Bechestedt, and A. Belabbes, J. Phys. : Condens. Matter **25**, 273201 (2013).

[55] P. Hohenberg, W. Kohn, Phys Rev **136**, B864 (1964); W. Kohn and L. J. Sham, Phys. Rev. **140**, A1133 (1965).

[56] S. Baroni, A. Dal Corso, S. de Gironcoli, P. Giannozzi, in https://www.pwscf.org.

[57] J. P. Perdew and A. Zunger, Phys. Rev. B **23**, 5048 (1981).

[58] A. Dal Corso, Phys. Rev. B **82**, 075116 (2010).

[59] H. J. Monkhorst and J. D. Pack, Phys. Rev. B **13**, 5188 (1976).

[60] S. Baroni, S. de Gironcoli, A. Dal Corso, and P. Giannozzi, Rev. Mod. Phys. **73**, 515 (2001).

[61]W. Wettling and J. Windscheif, Solid State Commun.**50**, 33 (1983).

[62] R. G. Greene, H. Luo, A. L. Ruoff, S. S. Trail, and F. J. DiSalvo, Jr., Phys. Rev. Lett.**73**, 2476 (1994).

[63] S. Das, R. Bhunia, S. Hussain, R. Bhar, B. R. Chakraborty, and A. K. Pal, Appl. Surface Science **353**, 439 (2015).

[64] M. Ferhat and A. Zaoui, Phys. Rev. B **73**, 115107 (2006).

[65] S. Cui, W. Feng, H. Hu, Z. Feng, and Y. Wang, Comput. Mater. Sci.**47**, 968 (2010).

[66] P. Lawaetz, Phys. Rev. B**5**, 4039 (1972).

[67] A. Menad, M. E. Benmalti, A. Zaoui, and M. Ferhat, Results in Physics, **18**, 103316 (2020).

[68] L. Hedin, Phys. Rev.**139**, A769 (1965).

[69]M. S. Hybersten and S. G. Louie, Phys. Rev. Lett.**55**, 1418 (1985); Phys. Rev. B **34**, 5390 (1986).

[70] P. Blaha, K. Schwarz, G. K. H. Madsen, D. Kvasnicka, and J. Luitz, WIEN2k: An Augmented Plane wave plus Local Orbitals Program for Calculating Crystal Properties (Vienna University of Technology, Austria, 2001).

[71] F. Tran, and P. Blaha, Phys. Rev. Lett.**102**, 226401 (2009).

[72] L. G. Ferreira, M. Marques, and L. K. Teles, Phys. Rev. B **78**, 125116 (2008).

[73] F. Matusalem, M. Marques, L. K. Teles, A. Fillippetti, and G. Cappellini, J. Phys.: Condens. Matter **30**, 365501 (2018).

[74] S. Dalui, S. Hussain, S. Varma, D. Paramanik, and A. K. Pal, Thin Solid Films **516**, 4958 (2008).

[75] S. Wang, S. F. Swingle, H. Ye, F. –R. F. Fan, A. H. Cowley, and A. J. Bard, J. Am. Chem. Soc.**134**, 11056 (2012).

[76] S. Hussain, S. Dalui, R. K. Roy, and A. K. Pal, J. Phys. D: Appl. Phys.**39**, 2053 (2006).

[77] V. Tiwari, I. Mal, S. K. Agnihotri, and D. P. Samajdar, Mat. Science in Semiconductor Processing, **122**, 105505 (2021).

[78] P. Carrier, and S. –H. Wei, Phys.Rev. B **70**, 035212 (2004).

[79] P. J. Gielisse, S. S. Mitra, J. N. Plendl, R. D. Griffis and L. C. Mansur, Phys.Rev. **155**, 1039 (1967).

[80] J. A. Sanjuro, E. L. –Cruz, P. Vogl, and M. Cardona, Phys. Rev. B **28**, 4579 (1983).

[81]C. Bungaro, K. Rapcewicz, and J. Bernholc, Phys. Rev. B **61**, 6720 (2000).

[82] N. Benyahia, A. Zaoui, D. Madouri, and M. Ferhat, J. Appl. Phys. **121**, 125701 (2017).

[83] F. Bernardini, V. Fiorentini, D. Vanderbilt, Phys.Rev. B **56**, R10024 (1997).

[84] A. Belabbes, J. Furthmüller, and F. Bechstedt, Phys. Rev B **87**, 035305 (2013).

[85] F. Bechstedt, H. Grossner, and J. Furthmüller, Phys. Rev B **62**, 8003 (2000).

Table Captions

Table I: Calculated equilibrium structural parameters, bulk modulus(B_0) and its pressure derivative (B'_0)for the 3C and 2H polytypes of boron III-V compounds.

Table II: Calculated minimum direct and indirect gaps, and spin-Orbit interaction (Δ_{SO}) of 3C boron III-V compounds.

Table III: Calculated minimum direct and indirect gaps, and spin-Orbit interaction (Δ_{SO}) of 2H boron III-V compounds

Table IV: Calculated phonon frequencies (cm^{-1}) at high symmetry points of the BZ of 3C boron III-V compounds.

Table V: Calculated phonon frequencies (cm^{-1}) at high symmetry points of the BZ of 2H boron III-V compounds.

Table VI: Calculated Born effective charge Z^* and high-frequency dielectric constant $\varepsilon(\infty)$ of 3C and 2H polytypes of boron III-V compounds

Table I

		a(Å)	c/a	u	B_0 (GPa)	B'_0
3C BP	Cal.	4.491			175.3	3.71
	Theory [16]	4.464			176	4
	Exp.	4.538[3]			173[61]	
2H BP	Cal.	3.158	1.695	0.3744	175.7	3.76
	Theory [19]	3.211	1.646	0.382	162.1	3.68
3C BAs	Cal.	4.744			147.7	4.02
	Theory [16]	4.726			147	3.00
	Exp.	4.774[3]			148[62]	3.9[62]
2H BAs	Cal.	3.339	1.656	0.3745	147.5	4.15
	Theory [19]	3.398	1.639	0.387	130.83	4.08
3C BSb	Cal.	5.188			113.2	4.27
	Theory [16]	5.201			109	4
	Exp. [63]	5.10				
2H BSb	Cal.	3.653	1.651	0.3746	114.1	4.40
	Theory [19]	3.737	1.625	0.388	98	4.64
3C BBi	Cal.	5.427			83.4	4.44
	Theory [64]	5.416			86.3	4.60
2H BBi	Cal.	3.819	1.649	0.3747	84.2	4.58
	Theory [65]	3.848	1.648		82.5	4.29

Table II

3C	Direct gap (eV)	Indirect gap (eV)	Δ_{SO}(meV)
BP			
mBJ-SO	4.064	1.763 (Γ→X)	38
LDA-1/2	4.050	1.874 (Γ→X)	32
BAs			
mBJ-SO	3.585	1.689 (Γ→X)	194
LDA-1/2	3.546	1.542 (Γ→X)	163
BSb			
mBJ-SO	2.826	0.937 (Γ→X)	324
LDA-1/2	2.834	1.036 (Γ→X)	290
BBi			
mBJ-SO	0.379	0.458 (Γ→L)	1129
LDA-1/2	0.580	0.852 (Γ→L)	909

Table III

2H	Direct gap (eV)	Indirect gap (eV)	Δ_{SO}(meV)
BP			
mBJ-SO	3.358	1.609 (Γ→K)	46
LDA-1/2	3.498	1.756 (Γ→K)	36
BAs			
mBJ-SO	2.745	1.537 (Γ→M)	372
LDA-1/2	2.444	1.566 (Γ→M)	181
BSb			
mBJ-SO	1.684	1.091 (Γ→M)	361
LDA-1/2	1.597	1.182 (Γ→M)	335
BBi			
mBJ-SO	0.187	0.714 (Γ→M)	1236
LDA-1/2	0.182	0.739 (Γ→M)	1025

Table IV

	Γ_{TO}	Γ_{LO}	X_{TA}	X_{LA}	X_{TO}	X_{LO}	L_{TA}	L_{LA}	L_{TO}	L_{LO}
BP	821.01	827.89	311.57	536.85	730.29	805.73	223.23	517.65	776.90	782.87
BAs	702.99	706.70	191.98	322.14	640.16	741.33	138.57	312.88	678.37	713.21
BSb	617.37	634.58	131.93	233.44	578.57	647.36	94.18	226.70	601.37	634.74
BBi	534.09	542.08	86.32	157.70	498.30	570.51	62.48	154.78	521.03	554.02

Table V

	E_2^l	B_1^l	A_1^{TO}	E_1^{TO}	E_2^h	B_1^h	A_1^{LO}	E_1^{LO}
BP	214.36	518.91	806.02	815.64	777.69	775.49	813.23	823.57
BAs	133.64	314.88	695.06	700.93	673.58	714.25	699.13	705.47
BSb	91.39	227.57	611.62	617.06	595.45	638.16	629.68	634.68
BBi	59.97	155.54	531.36	537.42	517.49	557.52	541.13	546.59

Table VI

		BP	**BAs**	**BSb**	**BBi**
$Z_{\perp}^{B}$	3C	-0.620	-0.510	-1.303	-1.110
	2H	-0.596	-0.489	-1.120	-0.981
$Z_{\parallel}^{B}$	3C	-0.620	-0.510	-1.303	-1.110
	2H	-0.650	-0.549	-1.360	-1.155
Z^{B}	2H	-0.614	-0.509	-1.250	-1.039
ΔZ^{B}	2H	0.088	0.118	0.192	0.167
$\epsilon_{\perp}(\infty)$	3C	9.226	9.723	11.147	16.978
	2H	8.697	9.006	10.232	13.265
$\varepsilon_{\parallel}(\infty)$	3C	9.226	9.723	11.147	16.978
	2H	9.578	10.064	11.570	15.239
$\varepsilon(\infty)$	2H	8.991	9.359	10.678	13.923
$\Delta\varepsilon(\infty)$	2H	0.098	0.113	0.125	0.142

Figure Captions

Figure1: Crystal structure of the 3C and 2H polytypes of boron III-V compounds.

Figure 2: Iso-energy lines of total energy $E(c, a)$ of 2Hpolytypes of boron III-V compounds.

Figure 3: Total energy versus volume of boron III-V compounds.

Figure4: 3C-mBJ band structure including spin-orbit coupling of boron III-V compounds.

Figure5: 2H-mBJ band structure including spin-orbit coupling of boron III-V compounds.

Figure6: 3C-Phonon band structure and phonon density of states (PhDoS) of boron III-V compounds.

Figure 7: 2H-Phonon band structure and phonon density of states (PhDoS) of boron III-V compounds.

Figure 1

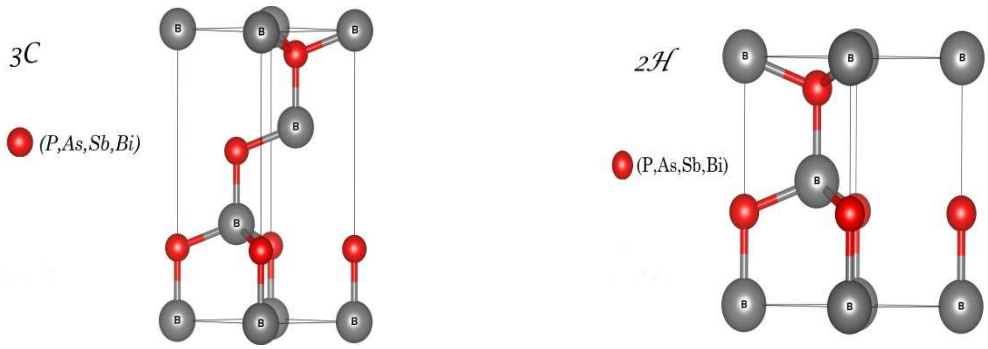

Figure 2

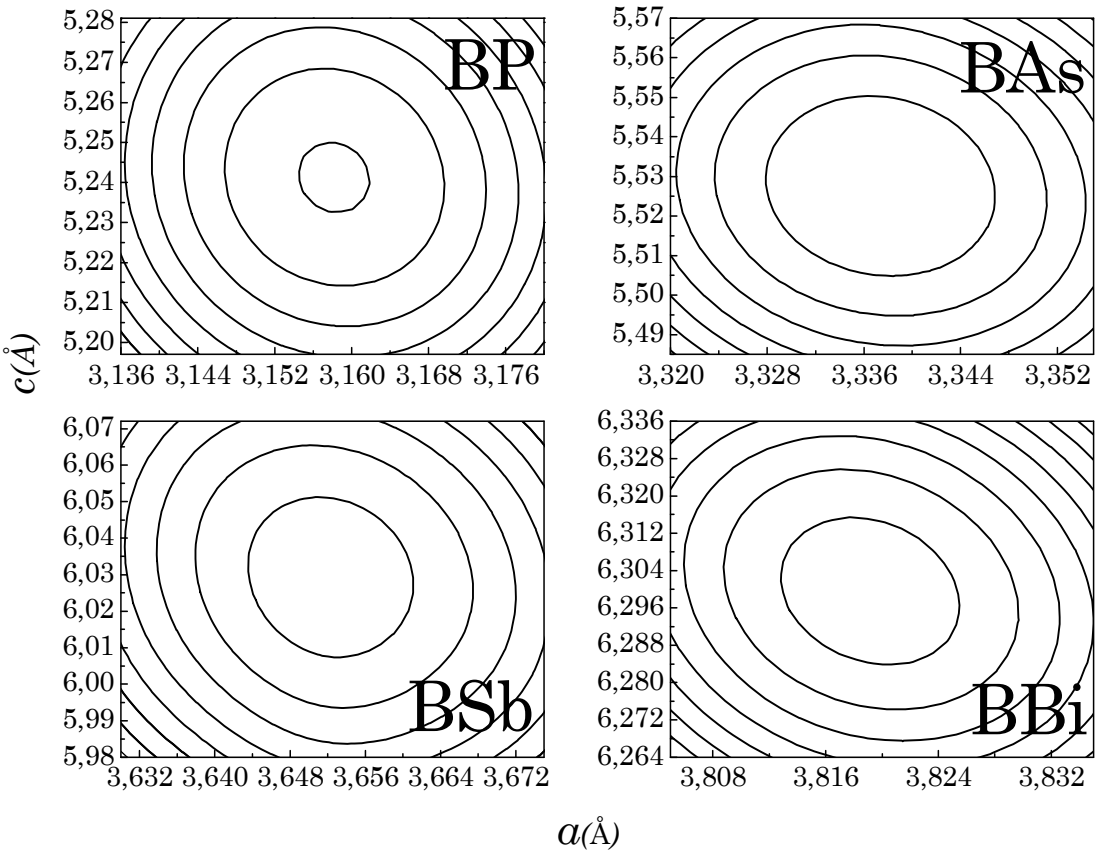

Figure 3

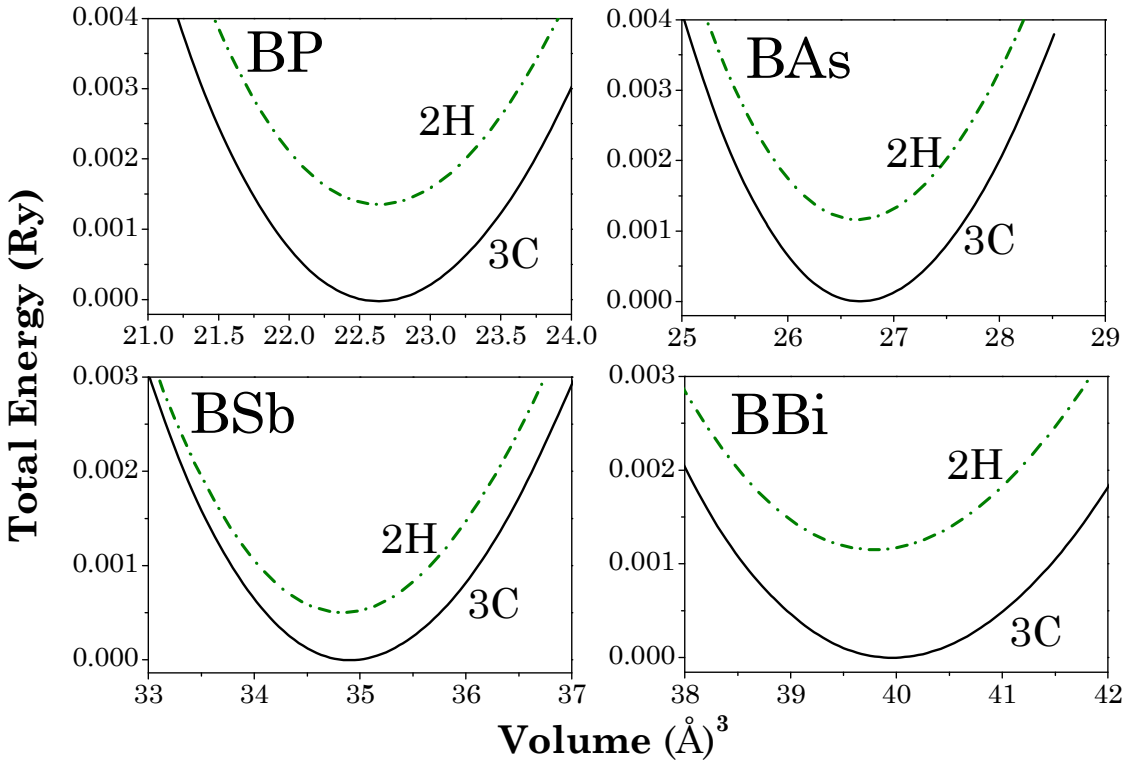

Figure 4

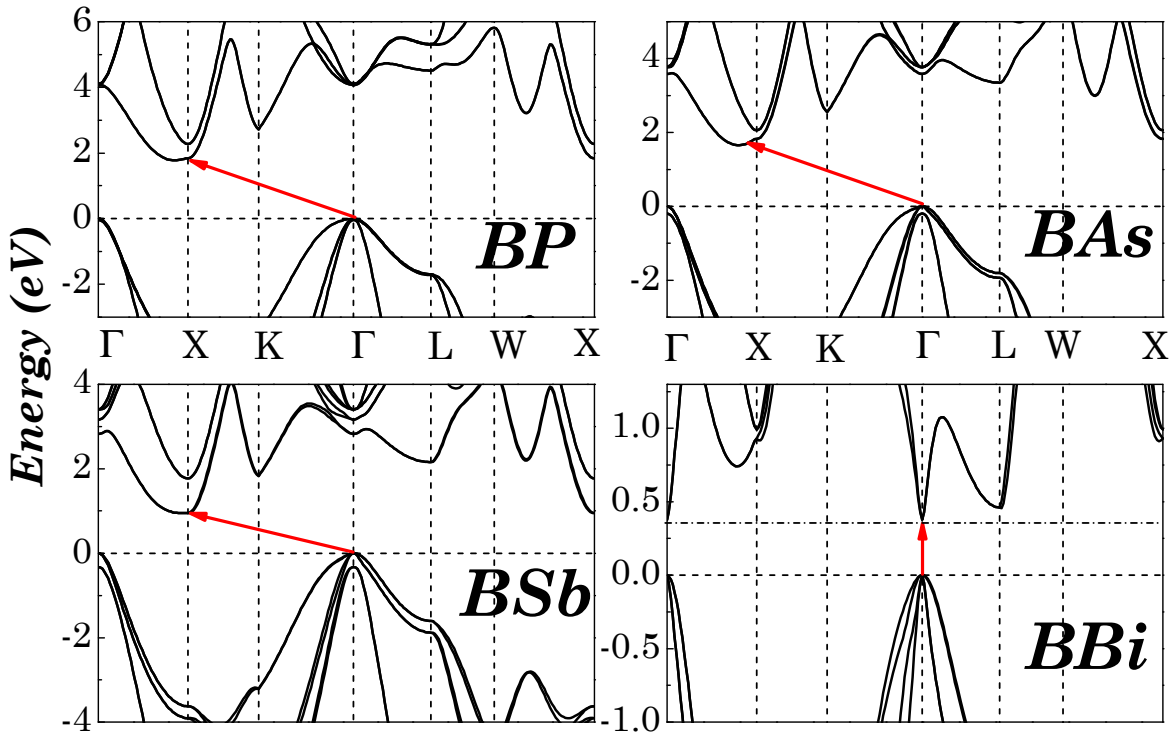

Figure 5

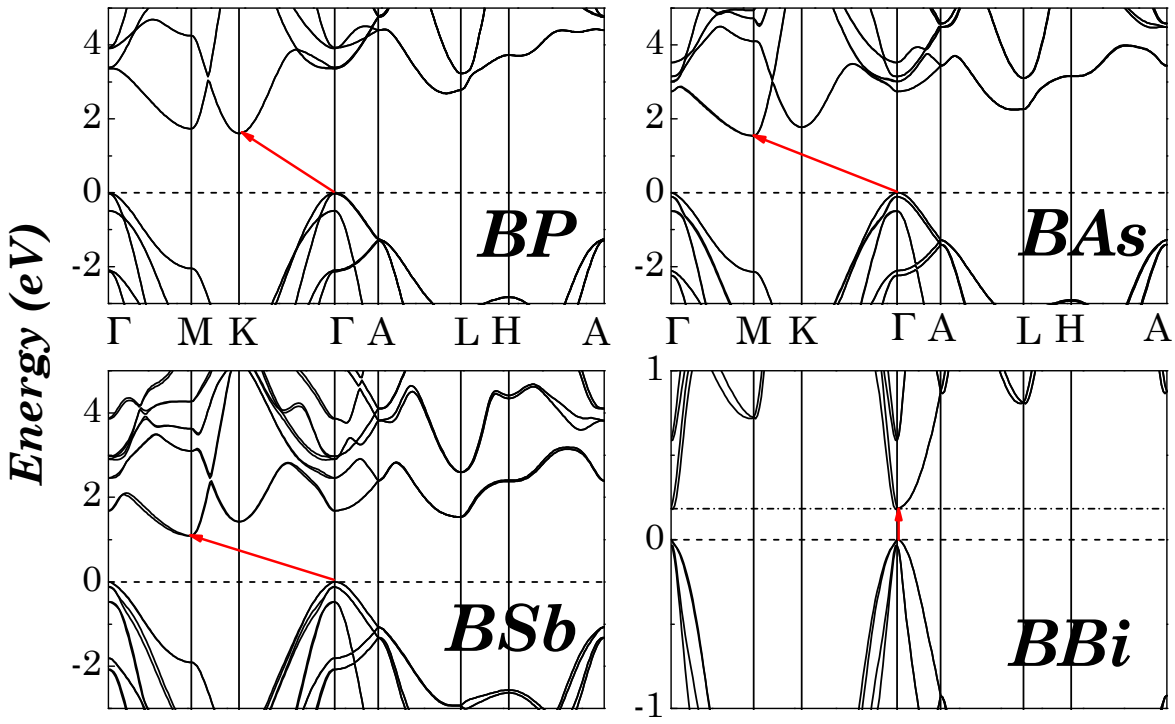
Energy (eV)
BP
BAs
BSb
BBi
Γ M K Γ A L H A
4
2
0
-2
1
-1

Figure 6

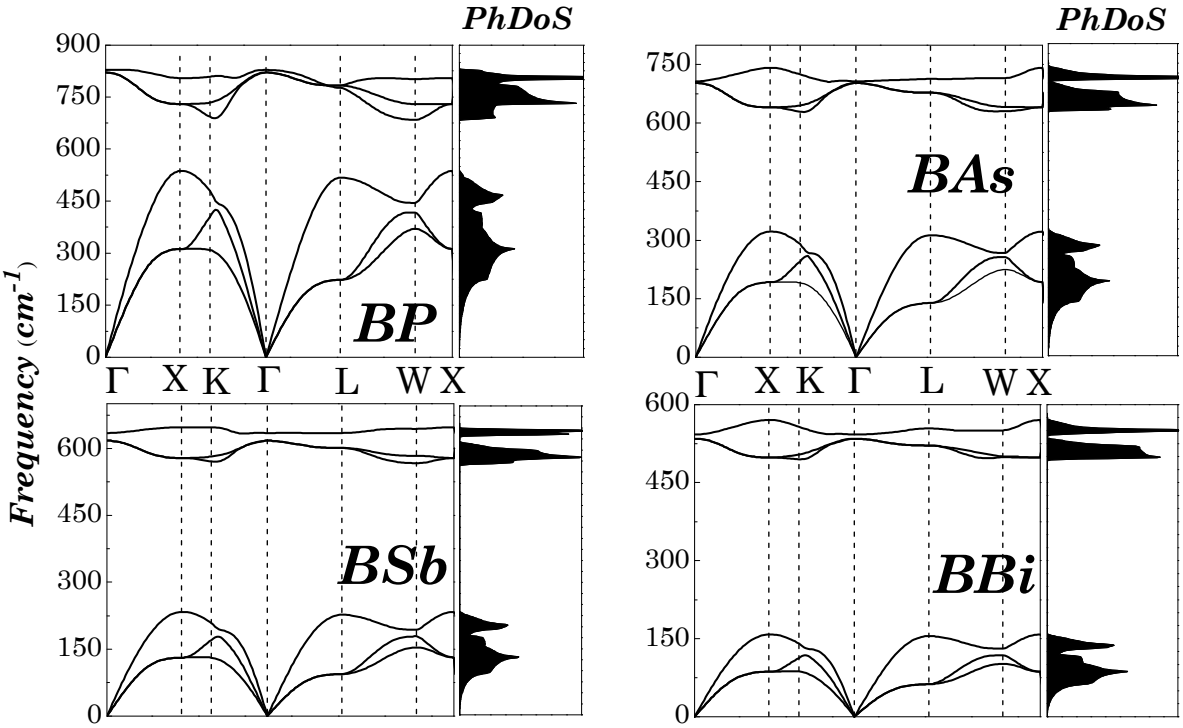
PhDoS
Frequency (cm-1)
BP
BAs
BSb
BBi
Γ X K Γ L W X
900
750
600
450
300
150
0

Figure 7